Geometric and Spectroscopic Study of Some Molecules Related to Eumelanins. 1. Monomers

L. E. Bolívar-Marinez,[†,‡] D. S. Galvão,[‡] and M. J. Caldas*[,†]

Instituto de Física, Universidade de São Paulo (USP), CP 66318, 05315-970, São Paulo, SP, Brazil, and Instituto de Física, Universidade Estadual de Campinas (UNICAMP), CP 6165, 13081-970, Campinas, SP, Brazil

Received: August 11, 1998; In Final Form: January 4, 1999

We have carried out ab initio and semiempirical PM3 (parametric method 3) and ZINDO (Zerner's intermediate neglect of differential overlap) calculations on neutral and charged 5,6-indolequinone and its reduced forms semiquinone and hydroquinone. These molecules are believed to compose the major part of the active material of eumelanin, a biological pigment present in illuminated and nonilluminated areas in living organisms. Our results show that these molecules can behave as electron acceptors and that their electronic behavior is consistent with that of the semiconductor models proposed for melanins. The relationship between electronic behavior and biological functions is also addressed.

I. Introduction

Melanins are a class of biological pigments widely spread in all *phila* from fungi to man.[1−4] The term *melanin* is purely descriptive, conveys no chemical information, and encompasses a family of pigments, roughly classified under the following:[5] *eumelanins*, black or dark-brown nitrogen-containing pigments; *phaeomelanins*, the pigment giving color to, for example, red hair and that also contains sulfur; *allomelanins*, occurring in the plant kingdom.

In this and in a following paper we will investigate only the eumelanins. There is a special interest in eumelanins because of their involvement in human pigmentation and related pathological conditions, such as albinism, vitiligo, and malignant melanoma.[1,6] They are also involved in some other pathologies as in the Parkinson's disease.[7]

From a biological point of view it is accepted[8,9] that the main skin protection against the biochemical devastation induced by solar exposure is provided by the melanin-containing granules (melanosomes) in the epithelial tissue.[3] However, the presence of melanins in nonilluminated areas of the body and the apparent preferential destruction of melanin-containing cells in the *substancia nigra* of the brain in Parkinsonism[7,10−13] suggest that melanins may have other biological functions besides mere photoprotection. In particular, it has been proposed[7] that melanins could act as deactivators of free radicals, produced or not by ionizing radiation.

Unfortunately, in what concerns structural and chemical composition, no melanin sample has been fully and unambiguously characterized yet, despite the enormous amount of experimental work. It has not been possible, up to now, to prove that two samples are identical, even for synthetic melanin samples prepared from the well-known precursors tyrosinase or DOPA (3,4-hydroxyphenylalanine).[15] One main difficulty is that melanins are insoluble in most organic solvents. In natural samples a protein matrix is always present and it is not exactly known to what extension the experimental procedures to isolate the pigment affect the polymeric structure. Indeed, the history of melanin research is unusual;[1−3] in contrast to other natural products the natural precursors and some intermediate products have been identified, but the chemical identity and structure of the pigment are not well-known. However, there is strong evidence[1−3] that the planar 5,6-indolequinone molecule (IQ) and/or their reduced forms semiquinone (SQ) and hydroquinone (HQ) (Figure 1) compose the major part of the active material

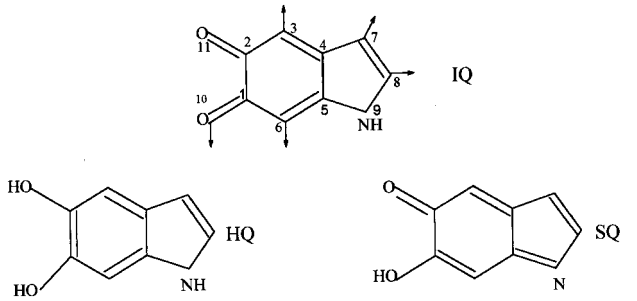

Figure 1. Schematic representation of the structures studied in this work: 5,6-indolequinone (IQ) and their reduced forms hydroquinone (HQ) and semiquinone (SQ). The active sites are indicated in the IQ.

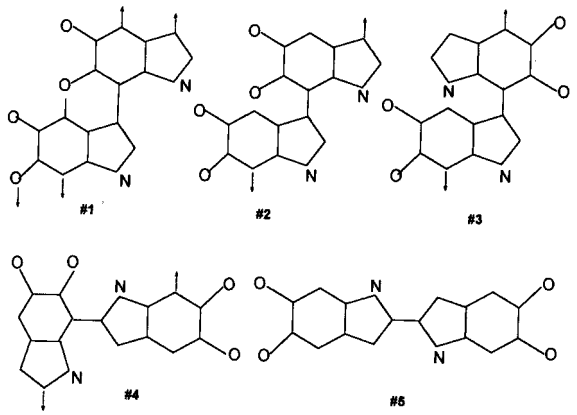

Figure 2. Schematic representation of eumelanin dimers. The arrows indicate the polymerization directions.

[†] Universidade de São Paulo.
[‡] Universidade Estadual de Campinas.

10.1021/jp983336s CCC: $18.00
Published on Web 03/25/1999

TABLE 1: Main Bond Lengths (Å) and Bond and Dihedral Angles (deg) for the Monomers Hydroquinone (Part a), Semiquinone (Part b), and Indolequinone (Part c), from Semi-empirical (PM3) and ab Initio (Gaussian 94) Methods

	semiempirical	ab initio					semiempirical	ab initio			
	PM3	6-31G(d)	6-31G(d.p)	6-311G(d)	6-311G(d.p)		PM3	6-31G(d)	6-31G(d.p)	6-311G(d)	6-311G(d.p)
						Part a					
C1−C2	1.433	1.416	1.416	1.415	1.415	C7−C4−C3	132.33	134.33	134.35	134.36	134.31
C3−C2	1.385	1.367	1.368	1.366	1.366	C8−C7−C4	107.81	106.72	106.72	106.71	106.71
C4−C3	1.401	1.405	1.404	1.404	1.404	N9−C5−C4	107.01	107.78	107.80	107.83	107.83
C5−C4	1.421	1.391	1.392	1.390	1.390	O10−C1−C2	123.35	116.39	116.42	116.52	116.42
C6−C5	1.403	1.399	1.399	1.399	1.398	O11−C2−C1	115.70	116.20	116.22	116.31	116.23
C7−C4	1.436	1.440	1.441	1.441	1.441	C4−C3−C2−C1	0.00	0.00	0.00	0.00	0.00
C8−C7	1.380	1.349	1.349	1.349	1.349	C5−C4−C3−C2	0.00	0.00	0.00	0.00	0.00
N9−C5	1.407	1.371	1.371	1.371	1.371	C6−C5−C4−C3	0.00	0.00	0.00	0.00	0.00
O10−C1	1.370	1.353	1.351	1.350	1.350	C7−C4−C3−C2	180.00	180.00	180.00	180.00	180.00
O11−C2	1.377	1.358	1.356	1.355	1.355	C8−C7−C4−C3	179.99	180.00	180.00	180.00	180.00
C3−C2−C1	121.64	120.41	120.40	120.33	120.36	N9−C5−C4−C3	179.99	180.00	180.00	180.00	180.00
C4−C3−C2	117.94	119.85	119.86	119.99	119.92	O10−C1−C2−C3	179.99	180.00	180.00	180.00	180.00
C5−C4−C3	120.03	118.86	118.86	118.83	118.87	O11−C2−C1−C6	179.99	180.00	180.00	180.00	180.00
C6−C5−C4	122.47	121.90	121.88	121.75	121.80						
						Part b					
C1−C2	1.509	1.513	1.514	1.515	1.516	C7−C4−C3	133.12	135.77	135.73	135.72	135.65
C3−C2	1.495	1.490	1.489	1.490	1.490	C8−C7−C4	107.03	104.96	104.95	104.97	104.96
C4−C3	1.334	1.324	1.324	1.323	1.323	N9−C5−C4	110.16	112.13	112.12	112.16	112.12
C5−C4	1.488	1.486	1.486	1.485	1.485	O10−C1−C2	113.05	112.37	112.36	112.38	112.34
C6−C1	1.356	1.330	1.330	1.329	1.329	O11−C2−C1	122.70	120.64	120.60	120.74	120.61
C7−C4	1.471	1.465	1.465	1.454	1.454	C4−C3−C2−C1	0.014	0.00	0.00	0.00	0.00
C8−C7	1.358	1.332	1.332	1.331	1.331	C5−C4−C3−C2	−0.003	0.00	0.00	0.00	0.00
N9−C5	1.318	1.269	1.269	1.267	1.267	C6−C1−C4−C3	−0.016	0.00	0.00	0.00	0.00
O10−C1	1.359	1.333	1.332	1.331	1.331	C7−C4−C3−C2	179.99	180.00	180.00	180.00	180.00
O11−C2	1.214	1.184	1.190	1.183	1.183	C8−C7−C4−C3	179.99	180.00	180.00	180.00	180.00
C3−C2−C1	116.71	117.96	118.00	117.80	117.88	N9−C5−C4−C3	179.99	180.00	180.00	180.00	180.00
C4−C3−C2	119.16	119.62	119.57	119.70	119.60	O10−C1−C2−C3	179.98	180.00	180.00	180.00	180.00
C5−C4−C3	122.59	121.07	121.10	121.15	121.19	O11−C2−C1−C6	179.98	180.00	180.00	180.00	180.00
C6−C5−C4	123.31	121.64	121.64	121.66	121.66						
						Part c					
C1−C2	1.539	1.556	1.556	1.559	1.559	C7−C4−C3	131.58	132.90	132.90	132.85	132.80
C3−C2	1.484	1.476	1.476	1.477	1.477	C8−C7−C4	108.62	107.20	107.10	107.13	107.12
C4−C3	1.340	1.332	1.331	1.330	1.329	N9−C5−C4	107.08	105.60	105.64	105.64	105.64
C5−C4	1.473	1.491	1.490	1.491	1.490	O10−C1−C2	120.97	118.81	118.79	118.83	118.79
C6−C5	1.344	1.334	1.334	1.334	1.333	O11−C2−C1	121.11	119.32	119.28		
C7−C4	1.462	1.461	1.461	1.461	1.461	C4−C3−C2−C1	3.24	0.00	0.00	0.00	0.00
C8−C7	1.356	1.333	1.333	1.332	1.332	C5−C4−C3−C2	0.41	0.00	0.00	0.00	0.00
N9−C5	1.439	1.373	1.373	1.373	1.373	C6−C5−C4−C3	2.34	0.00	0.00	0.00	0.00
O10−C1	1.215	1.191	1.191	1.185	1.185	C7−C4−C3−C2	179.87	180.00	180.00	180.00	180.00
O11−C2	1.214	1.190	1.190	1.184	1.184	C8−C7−C4−C3	179.23	180.00	180.00	180.00	180.00
C3−C2−C1	117.99	118.30	118.30	118.17	118.19	N9−C5−C4−C3	174.84	180.00	180.00	180.00	180.00
C4−C3−C2	119.37	119.50	119.4	119.49	119.41	O10−C1−C2−C3	174.65	180.00	180.00	180.00	180.00
C5−C4−C3	122.19	121.53	121.57	121.62	121.66	O11−C2−C1−C6	174.72	180.00	180.00	180.00	180.00
C6−C5−C4	123.59	124.40	124.42	124.35	124.40						

of the biological pigment. It is believed that eumelanins are a product of the copolymerization of these molecules and both residual precursors and intermediate products.[2]

There are only few physical studies of eumelanins, and they seem to corroborate the hypothesis of a polymeric amorphous material.[16−20] X-ray studies[21] indicate the existence of planar sections (as would be expected from IQ polymers) stacked with an interplanar separation of 3.4 Å. No long-range order is detected, whatever the source or method of preparation of melanin samples. The effect of threshold switching, typical of the electrical behavior of amorphous materials, is found in experiments with synthetic eumelanin solid pellets.[22] Supporting these "solid-state" signatures we have (a) the optical absorption spectrum, which shows a monotonic rise after a threshold around 1.5 eV, with an ill-defined shoulder at 0.7 eV and (b) the presence of an EPR (electron paramagnetic resonance) line characteristic of free radicals or, in semiconductor language, highly localized (dangling-bond-like) defect states. That melanins could act as an intrinsic semiconductor was first proposed on theoretical grounds by Longuet-Higgins in 1960[23] and received additional support based on simple Hückel calculations on monomers by Pullman and Pullman in 1961.[24]

Pullman's model was later rejected by Blois and co-workers[25] on the basis of the EPR data, which seemed to rule out the presence of π-electron delocalized bands. However, two of us have later demonstrated,[17−19] on the basis of Hückel electronic structure calculations but for long oligomers, that the EPR data are not inconsistent with delocalized bands provided the model takes into account the crucial role of chain ends, which act as deep electron traps. This materials science interpretation of the magnetic resonance contrasts with the notion that a localized EPR signal must necessarily be produced by a broken (nonsaturated) bond. Indeed, an unpaired electron captured at any highly localized state may produce a similar signal, and such a state was found for the oligomers.[17] Thus, for the first time, a semiconductor model for eumelanins was presented based on actual electronic structure calculations for polymers of IQ and its reduced forms SQ and HQ. Even using an extremely simple model, we were able to explain some of the properties of the pigment, such as the stabilization of free radicals (through electron trapping at deep defect states) and the behavior of paramagnetism with temperature. It remained to be proved that the predictions of such simple calculations would hold in the light of more sophisticated studies. Surprisingly, up to now no

TABLE 2: Root-Mean-Square Deviations, Obtained from the Comparison between PM3 and ab Initio (Gaussian 94) Methods with Different Basis Sets for the Hydroquinone, Semiquinone, and Indolequinone Monomers[a]

	PM3 6-31G(d)	PM3 6-31G(d,p)	PM3 6-311G(d)	PM3 6-311G(d,p)
Hydroquinone				
bond length	0.0091	0.0092	0.0095	0.0095
bond angle	0.901	0.905	0.914	0.926
dihedral angle	0	0	0	0
Semiquinone				
bond length	0.0078	0.0120	0.0078	0.0121
bond angle	0.796	0.794	0.795	0.794
dihedral angle	0.005	0.005	0.005	0.005
Indolequinone				
bond length	0.0099	0.0099	0.0108	0.0108
bond angle	0.461	0.459	0.542	0.542
dihedral angle	1.42	1.42	1.42	1.42

[a] These results are for the data shown in Table 1. Bond lengths are in angstroms and angles in degrees.

detailed calculations beyond the Hückel level have been published on these experimentally well-studied materials.

The use of the simple π-electron Hückel theory in our previous work[17−19] was dictated by the need to treat relatively long polymeric chains (up to 10 monomeric units) and to survey a large number of structures, which precludes the use of good quality ab initio methods or even sophisticated semiempirical methods. However, the use of sophisticated methods to treat geometrical and spectroscopic aspects of IQ, SQ, and HQ (neutral and in charge states -2, -1, $+1$, and $+2$) and their dimers (Figure 2) is feasible and is the subject of the present study. The use of methods that include all valence electrons will allow us to get more refined results, to evaluate the applicability of Hückel theory, to validate the Hückel predictions, and to analyze some aspects that cannot be obtained at all from Hückel calculations. Two results of special relevance can be extracted from these calculations: whether the optical absorption spectra of monomers and dimers are consistent with the available experimental data and if they behave as electron acceptors. Besides that, the inclusion of all valence electrons in the calculations allows us to estimate the energetic cost involved in the process of dimerization for the many possible structural configuration models (Figure 2). This is not possible within the Hückel framework, where only the π-electrons is taken into account.

In this paper we only consider the IQ and its reduced forms SQ and HQ, as well as their ions; the process of polymerization will be the subject of a following paper. The methodology we use is described in section 2. In section 3 we discuss our results, and finally in section 4 we present a summary and our main conclusions.

2. Methodology

Experimental data on the geometry of the molecules shown in Figure 1 are not available. To carry out a comparative study of these molecules, it is necessary to perform geometry optimizations. As mentioned before, we intend to investigate the energetic cost associated with adding/removing one and two electrons to/from the neutral structures. This cost can be estimated through the difference in the heats of formation for neutral and ionic molecules. So we need also to carry out full geometry optimizations for the IQ, SQ, and HQ in the charge states -2, -1, 0, $+1$, and $+2$ (and subsequently for their dimers).

Considering the number and size of these molecules, the use of good quality ab initio methods for all of them is costly

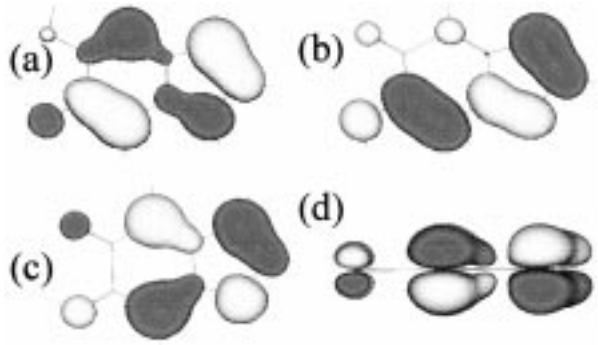

Figure 3. Spatial representation of highest occupied molecular orbital (HOMO) for the (a) hydroquinone, (b) semiquinone, and (c, d) indolequinone molecules. The clear π-character of these states can be seen from (d).

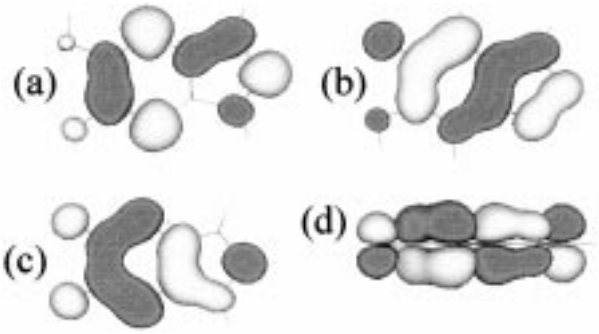

Figure 4. Spatial representation of lowest unoccupied molecular orbital (LUMO) for the (a) hydroquinone, (b) semiquinone, and (c, d) indolequinone molecules. The clear π-character of these states can be seen from (d).

prohibitive but feasible within the framework of sophisticated semiempirical methods. To establish the reliability and quality of our semiempirical calculations, we have also carried out ab initio calculations for the neutral states of IQ, SQ, and HQ, including an analysis of different basis sets (6-31G(d), 6-31G(d,p), 6-311G(d), and 6-311G(d,p)). We have used for that the GAUSSIAN-94 program.[26]

Sophisticated semiempirical methods such as MNDO (modified neglect of differential overlap),[27] AM1 (Austin method 1),[28] and PM3 (parametric method 3)[29] provide a good balance between quality and computational effort and have been extensively and successfully used to treat organic molecules. The AM1 method has been developed in an attempt to correct some of the MNDO weaknesses. In AM1, as in MNDO, all two-center electron−nuclear attraction integrals are retained, but the tendency of MNDO to overestimate the repulsion between neutral atoms has been corrected by a suitable modification of the Hamiltonian in the core repulsion function.[28] More recently, a new parametrization for these methods, the PM3,[30] has been introduced in order to improve MNDO and AM1 results. Basically, PM3 maintains the same AM1 Hamiltonian with a new set of parameters. However, although there seems to be a consensus that AM1 is in general better than MNDO, there is an ongoing debate about the relative merits of AM1 and PM3,[31] and in this work we have used the PM3 method. Results are then compared with those from the ab initio calculations.

Geometrical features for the ground state such as bond lengths, bond angles, dihedral angles, heats of formation, dipole moment values, etc. are well described by PM3, but the energies of the electronic transitions to excited states are overestimated, as expected from a zero differential overlap (ZDO)[32] Hartree−Fock method without configuration interaction corrections. Thus,

TABLE 3: Main Bond Lengths (Å) and Bond and Dihedral Angles (deg) of the Hydroquinone Monomer in Its Neutral and Charged States for Fully Optimized (Top) and Planar (Bottom) Geometries

charge	−2	−1	0	+1	+2	charge	−2	−1	0	+1	+2
					Part a						
C_2-C_1	1.383	1.395	1.433	1.469	1.460	$C_8-C_7-C_4$	109.8	108.6	107.8	107.7	107.5
	1.381	1.395	1.435	1.469	1.468		109.8	108.6	107.8	107.7	107.6
C_3-C_2	1.412	1.411	1.386	1.426	1.371	$N-C_5-C_4$	106.2	106.7	107.0	107.5	105.3
	1.414	1.411	1.387	1.426	1.373		106.3	106.7	107.1	107.5	105.3
C_6-C_5	1.378	1.391	1.403	1.417	1.344	$O_1-C_1-C_2$	124.8	124.1	123.3	114.7	125.5
	1.379	1.391	1.403	1.417	1.343		120.0	124.1	116.3	114.7	116.8
$N-C_5$	1.401	1.404	1.407	1.367	1.475	$O_2-C_2-C_1$	117.6	117.3	115.7	115.9	112.6
	1.400	1.404	1.407	1.367	1.478		117.9	117.3	116.1	115.9	113.4
$O-C_1$	1.401	1.386	1.370	1.349	1.361	$C_5-C_4-C_3-C_2$	0.00	0.00	0.00	0.00	0.00
	1.403	1.386	1.368	1.349	1.353		0.00	0.00	0.00	0.00	0.00
$C_3-C_2-C_1$	124.1	122.5	121.6	120.8	121.7	$C_8-C_7-C_4-C_3$	180.00	180.00	180.00	180.00	180.00
	123.7	122.5	121.2	120.8	121.1		180.00	180.00	180.00	180.00	180.00
$C_4-C_3-C_2$	116.6	117.1	117.9	117.9	118.5	$N-C_5-C_4-C_3$	180.00	180.00	180.00	180.00	180.00
	116.9	117.1	118.2	117.9	119.1		180.00	180.00	180.00	180.00	180.00
$C_6-C_5-C_4$	124.7	123.6	122.5	121.8	124.1	$O_1-C_1-C_2-C_3$	180.00	180.00	180.00	180.00	180.00
	124.5	123.6	122.3	121.8	123.8		180.00	180.00	180.00	180.00	180.00
$C_7-C_4-C_3$	133.2	132.6	132.3	132.3	132.1	$O_2-C_2-C_1-C_6$	180.00	180.00	180.00	180.00	180.00
	133.2	132.6	132.3	132.3	132.2		180.00	180.00	180.00	180.00	180.00
					Part b						
C_2-C_1	1.463	1.488	1.51	1.530	1.547	$N-C_5-C_4$	109.8	110.1	110.2	108.3	106.8
	1.463	1.488	1.51	1.530	1.547		109.8	110.1	110.2	108.3	106.8
C_4-C_3	1.400	1.371	1.334	1.342	1.356	$O_1-C_1-C_2$	116.5	114.7	113.0	113.8	115.0
	1.400	1.371	1.334	1.342	1.356		116.5	114.7	113.0	13.8	115.0
C_7-C_4	1.427	1.442	1.471	1.456	1.437	$O_2-C_2-C_1$	122.0	122.0	122.7	121.9	121.4
	1.427	1.442	1.471	1.456	1.437		122.0	122.0	122.7	121.9	121.4
$N-C_5$	1.416	1.365	1.318	1.385	1.446	$C_5-C_4-C_3-C_2$	0.00	0.00	0.00	0.00	0.00
	1.416	1.365	1.318	1.385	1.446		0.00	0.00	0.00	0.00	0.00
O_1-C_1	1.393	1.376	1.359	1.312	1.273	$C_6-C_1-C_2-C_3$	0.00	0.00	−0.02	0.00	0.00
	1.393	1.376	1.359	1.312	1.273		0.00	0.00	0.00	0.00	0.00
O_2-C_2	1.276	1.240	1.214	1.207	1.203	$C_8-C_7-C_4-C_3$	179.99	179.99	179.99	179.99	179.99
	1.276	1.240	1.214	1.207	1.203		180.00	180.00	180.00	180.00	180.00
$C_3-C_2-C_1$	115.9	116.5	116.7	116.6	116.7	$N-C_5-C_4-C_3$	179.99	179.99	179.99	179.99	179.99
	115.9	116.5	116.7	116.6	116.7		180.00	180.00	180.00	180.00	180.00
$C_4-C_3-C_2$	120.9	119.8	119.2	118.6	118.6	$O_1-C_1-C_2-C_3$	180.00	180.00	179.98	180.00	179.99
	120.9	119.8	119.2	118.6	118.6		180.00	180.00	180.00	180.00	180.00
$C_8-C_7-C_4$	106.4	106.7	107.0	106.8	106.9	$O_2-C_2-C_1-C_6$	179.99	180.00	179.98	180.00	179.99
	106.4	106.7	107.0	106.8	106.9		180.00	180.00	180.00	180.00	180.00
					Part c						
C_2-C_1	1.524	1.526	1.539	1.534	1.535	$C_8-C_7-C_4$	109.4	108.7	108.6	107.9	106.8
	1.528	1.529	1.540	1.535	1.535		109.1	108.6	108.5	107.9	106.8
C_4-C_3	1.416	1.376	1.340	1.355	1.39	$N-C_5-C_4$	108.3	107.8	107.1	105.7	105.6
	1.415	1.378	1.341	1.355	1.389		106.9	106.6	106.2	105.7	105.6
C_7-C_4	1.421	1.447	1.462	1.435	1.403	$O_1-C_1-C_2$	121.6	121.0	121.0	122.0	122.2
	1.418	1.443	1.461	1.435	1.403		121.3	120.8	120.8	121.9	121.8
$N-C_5$	1.441	1.444	1.440	1.434	1.438	$C_5-C_4-C_3-C_2$	0.03	0.39	0.41	1.60	3.63
	1.404	1.416	1.419	1.435	1.438		0.00	0.00	0.00	0.00	0.00
$O-C_1$	1.258	1.236	1.215	1.207	1.203	$C_8-C_7-C_4-C_3$	177.92	178.89	179.23	178.43	178.00
	1.260	1.237	1.216	1.208	1.204		180.00	180.00	180.00	180.00	180.00
$C_3-C_2-C_1$	118.6	118.5	118	117.9	117.9	$N-C_5-C_4-C_3$	176.62	176.30	174.84	178.34	177.89
	118.9	118.7	118.2	118.2	118.7		180.00	180.00	180.00	180.00	180.00
$C_4-C_3-C_2$	120.5	119.7	119.4	119.1	118.2	$O_1-C_1-C_2-C_3$	179.10	178.95	174.65	167.37	159.67
	120.6	119.7	119.5	119.2	118.7		180.00	180.00	180.00	180.00	180.00
$C_7-C_4-C_3$	132.5	131.7	131.6	131.2	130.6	$O_2-C_2-C_1-C_6$	179.85	179.38	174.72	167.32	159.36
	132.9	132.0	131.7	131.2	130.5		180.00	180.00	180.00	180.00	180.00

it is necessary to use a method specially designed to obtain a more realistic description of electronic transitions (simulated absorption spectra). We have chosen INDO−CI (intermediate neglect of differential overlap−configuration interaction),[33] which retains also the exchange integrals for same-atom orbitals. We have used a version properly calibrated to treat organic compounds (ZINDO−CI, Zerner's INDO).[34]

We have carried out ZINDO−CI calculations using an average of 200 configurations (singlet/triplet) with the geometry obtained from PM3 calculations. The ZINDO−CI energy transitions and oscillator strengths are Gaussian enveloped and properly weighted to simulate the optical absorption spectra. This methodology has been used with success in the description of organic molecules.[35]

3. Results and Discussions

In Table 1 we present a summary of the geometrical data from PM3 calculations and compared it to ab initio Gaussian results with different basis sets. Main bond lengths and bond and dihedral angles are indicated. As we can see from the table, there are only small differences at different ab initio levels; the structures are basically planar with only the nitrogen and oxygen atoms for indolequinone (and consequently, the hydrogen atoms attached to the nitrogen atom) departing from planarity. Even for IQ the departure from planarity is very small. These results imply that $\sigma-\pi$ splitting is really to be expected.

There is good agreement between ab initio and PM3 results. This agreement can be better evaluated from the root-mean-

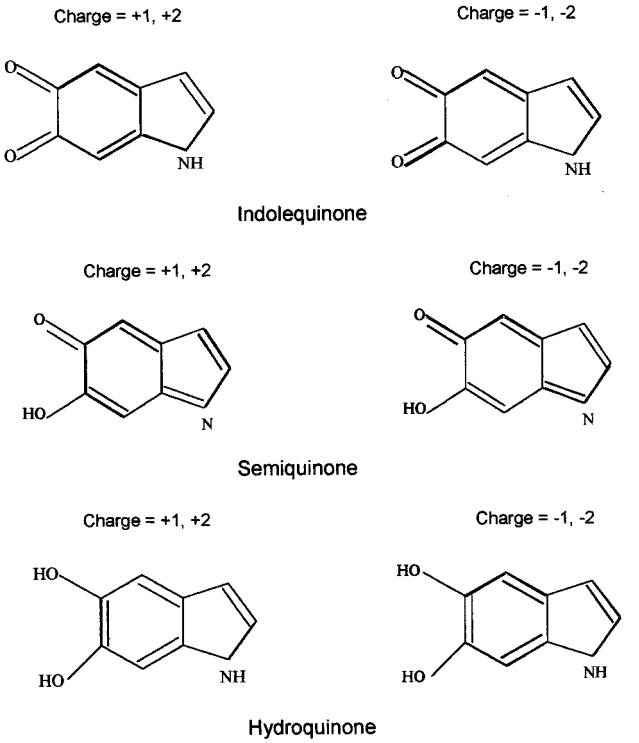

Figure 5. Schematic representation of geometrical changes induced by excess/lack of charge (negative ions: −1 and −2) for the indolequinone, semiquinone and hydroquinone molecules. The darker bonds indicate where the changes are more significant.

square deviations indicated in Table 2. These results indicate, as we expected, that PM3 provides very reliable geometries for these monomers. The calculations for the ionic structures, which are much more CPU-time-consuming, were thus calculated only using the PM3 method.

Since the molecules have basically planar conformations, the HOMO−LUMO transition will have a clear $\pi \rightarrow \pi^*$ character for all molecules (see Figures 3 and 4). But apart from that, this character is very different for the three cases, since the nodal pattern for the HOMO is similar for HQ and IQ, but the LUMO shows some similarity for SQ and IQ. It can be seen that the LUMO for IQ bears a large orbital contribution from the four C atoms in the quinone ring closer to the O atoms and from the O atoms themselves; in fact, for both IQ and SQ the LUMO spreads much more over adjacent atoms, while for HQ it shows more nodes and bears relatively fewer contributions from the oxygen atomic orbitals. From this analysis, we can expect quite different electronic behavior, and the results from oligomeric Hückel calculations are consistent with these results.[17−19]

In Table 3 we show a summary of the PM3 geometrical data for the molecules and their ions (−2, −1, +1, and +2 charge states, respectively). Since X-ray studies indicate the existence of stacked planar sections, for comparison purposes we have also carried out PM3 geometrical optimizations under constrained planarity. As we can see from the tables and from Figure 5, the geometrical changes induced by excess/lack of charge show few overall trends. The only definite trend is that the O atoms are the most affected by excess charge, bond lengths increasing (decreasing) with negative (positive) charge. These observations are valid for free and planar constrained structures, as we can see from Table 3. Another overall effect is that planarity increases both with negative and positive charges for SQ and HQ, while for IQ there is an increase or decrease in planarity for negative or positive charge, respectively.

TABLE 4: PM3 Results for Hydroquinone (HQ), Semiquinone (SQ), Indolequinone (IQ), and Semiquinone Radical (SQR), Respectively, in Their Neutral and Charged States for Fully Optimized (Top) and Planar Geometries (Bottom, Not Shown for SQR)[a]

	charge	− 2	−1	0	+1	+2
HQ	HF	60.976	−51.521	−45.907	137.068	421.702
	(kcal/mol)	60.918	−51.521	−43.765	137.068	426.672
	DM	3.917	0.649	1.542	2.677	5.584
	(D)	3.233	0.649	2.967	2.677	7.848
	ΔHF	106.883	−5.614		182.975	467.609
	(kcal/mol)	104.683	−7.756		180.833	470.437
SQ	HF	−2.265	−53.468	4.624	204.044	505.203
	(kcal/mol)	−2.265	−53.468	4.624	204.044	505.203
	DM	2.906	1.296	1.172	1.735	2.462
	(D)	2.906	1.296	1.172	1.735	2.462
	ΔHF	−6.889	−58.092		199.42	500.579
	(kcal/mol)	−6.889	−58.092		199.42	500.579
IQ	HF	5.353	−57.589	−8.929	183.159	491.008
	(kcal/mol)	8.530	−54.946	−7.229	183.166	491.046
	DM	8.232	7.035	5.821	9.497	12.284
	(D)	9.135	7.730	6.454	9.523	12.358
	ΔHF	14.282	−48.660		192.088	498.937
	(kcal/mol)	15.759	−47.717		190.395	498.275
SQR	HF		−47.792	24.479	224.594	
	(kcal/mol)					
	DM		1.757	4.155	7.151	
	(D)					
	ΔHF		−72.271		200.115	
	(kcal/mol)					

[a] We show the heat of formation (HF), dipole moments (DM), and energy differences (ΔHF) between the charged and neutral species (a negative ΔHF means that that particular charge state is stable compared to the neutral state).

In Table 4 we show another summary of PM3 results for neutral and ionic molecules (free and planar constrained) related to the energetics of adding/removing charge. The values for the heat of formation (HF), dipole moment (DM), and the difference in heats of formation between the neutral and the ionic structures (ΔHF) are presented. Analyzing first the absolute heats of formation (HF), we see that neutral HQ and IQ are stable forms but SQ is (slightly) unstable. All singly negative charged forms are stable, and SQ is at the limit of stability even in the doubly negative charge state; all results for the unpaired-electron systems were obtained in the restricted Hartree−Fock approximation. These results support the hypothesis that SQ is a *stable radical* and does not exist in the neutral state. Also, since at neutral physiological-relevant pH, the semiquinone is present in its anionic dissociated form, it is interesting to analyze the incompletely saturated SQ (see Figure 1) for which the oxygen-bonded hydrogen is also removed from the structure ($C_8H_4NO_2$). We will call this structure the semiquinone radical (SQR) following common use. Results for the SQ radical are in the last line of Table 4, and we see that also in this form the structure is unstable in the positive and neutral charge states and stable in the negatively charged state.

Then, through the ΔHF differences we estimate the cost of adding/removing electrons from/to neutral molecules. As we can see from Table 4, there is an energetic gain for all three molecular forms with the capture of one electron, this gain increasing from HQ to IQ, and even the capture of a pair of electrons is energetically favorable to SQ. All results for the unpaired-electron systems were obtained in the restricted Hartree−Fock approximation so that the relative stability of the anions is at worst *underestimated* (for the radical we also calculated the neutral form in the ultra-Hartree−Fock approximation, and still in that case the negative form is stable over the neutral form by 60.97 kcal/mol).

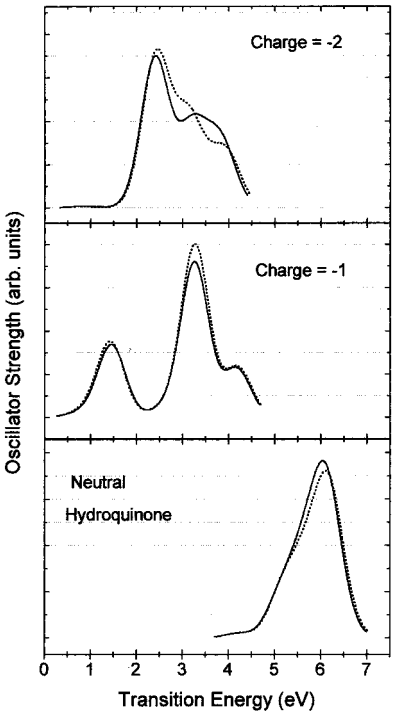

Figure 6. Simulated optical absorption spectra of the hydroquinone monomer and their negative ions (−1 and −2). These curves were obtained from the optical transition spectrum enveloped by normalized Gaussian functions weighted by the calculated oscillator strengths. The dashed and full lines refer to fully optimized and planar constrained conformations, respectively.

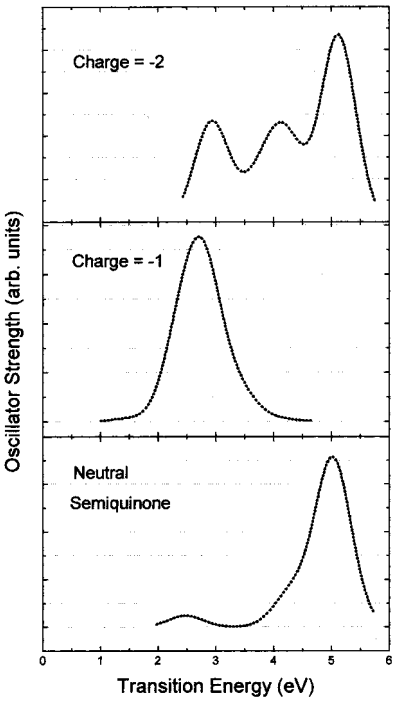

Figure 7. Simulated optical absorption spectra of the semiquinone monomer and their negative ions (−1 and −2). These curves were obtained from the optical transition spectrum enveloped by normalized Gaussian functions weighted by the calculated oscillator strengths. The dashed and full lines refer to fully optimized and planar constrained conformations, respectively.

The energetic cost to remove one electron is relatively high (∼200 kcal/mol), and the cost to remove a pair of electrons is definitively prohibitive (∼500 kcal/mol). In other words, this suggests that all eumelanin monomers are strong electron acceptors.

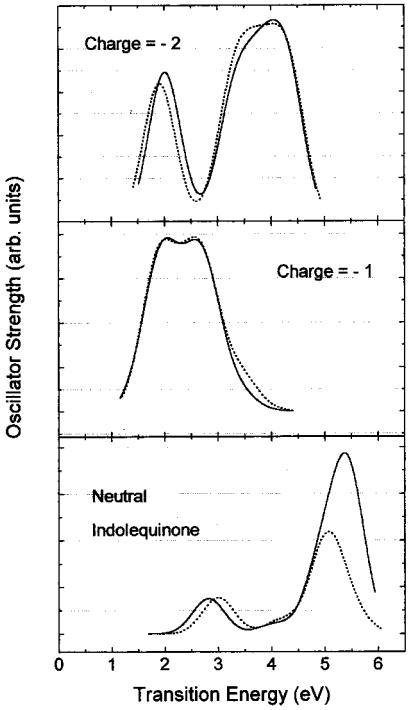

Figure 8. Simulated optical absorption spectra of the indolequinone monomer and their negative ions (−1 and −2). These curves were obtained from the optical transition spectrum enveloped by normalized Gaussian functions weighted by the calculated oscillator strengths. The dashed and full lines refer to fully optimized and planar constrained conformations, respectively.

At this point it is useful to stress that most π-conjugated structures are good electron donors (or, in semiconductor language, hole conductors[16]), and our results for all monomers (M) suggest strong acceptor activity; that is, neutral species are unstable against electron capture:

$$E(\mathrm{M}^0 + \mathrm{e}^-) \rightarrow E(\mathrm{M}^-) + \delta E, \quad \delta E \cong 50 \text{ kcal/mol}$$

where E refers to the energy of the neutral monomer (M^0) and its anion (M^-).

Now, a singly negative monomer would present the appearance of a stable radical in the sense that the state is localized, and the spin is one-half ($S = {}^1/_2$). The semiquinone radical SQR, on the other hand, is unstable as an $S = {}^1/_2$ system and is stabilized as an anion, but in that case the molecule is nonmagnetic with spin $S = 0$. The electron acceptor properties of melanins are discussed in detail in refs 24 and 36.

It is interesting to observe that although the molecules are virtually planar, there is considerable variation in the dipole moment values (DM) for the IQ and HQ molecules when full planarity is imposed. Also, there is considerable DM variation, although without a specific pattern, for the ionic structures. We may then expect different light-interaction properties, as we show next.

In Figures6−8 we show the simulated optical absorption spectra for the IQ, SQ, and HQ molecules and their negative ions (−1 and −2). As we can see from these figures, in the neutral state the threshold for optical absorption is around ∼2.0 eV for the IQ and SQ, while in the case of the HQ it is roughly 3.8 eV. But in the case of the ions, all molecules began to absorb at around 1.0 eV, and in particular for HQ, this value is around 0.75 eV.

TABLE 5: Most Relevant CI Expansion Coefficients for Fully Optimized (Top) and Planar (Bottom) Monomers of Melanin, Hydroquinone (HQ), Semiquinone (SQ) and Indolequinone (IQ) in Their Neutral and Charged Statesa[a]

		first transition			strongest transition		
system/charge		energy (eV)	oscillattor strength	main contributions	energy (eV)	oscillattor strength	main contributions
HQ	−2	0.84	0.0017	$-0.828\ \|H \rightarrow L\rangle\ 0.324\ \|H \rightarrow L+1\rangle$	2.43	0.1775	$-0.824\ \|H \rightarrow L\rangle\ 0.340\ \|H \rightarrow L+1\rangle$
		0.90	0.0021	$0.567\ \|H \rightarrow L, L+1\rangle\ 0.560\ \|H \rightarrow L+1\rangle$	2.41	0.1731	$0.567\ \|H \rightarrow L+1\rangle\ 0.556\ \|H \rightarrow L, L+1\rangle$
	−1	0.77	0.0044	$-0.821\ \|H \rightarrow L\rangle\ 0.469\ \|H \rightarrow L+1\rangle$	3.27	0.1495	$0.818\ \|H \rightarrow L\rangle\ -0.474\ \|H \rightarrow L+1\rangle$
		0.81	0.0044	$0.666\ \|H\text{-}1 \rightarrow H\rangle\ -0.293\ \|H\text{-}2 \rightarrow H\rangle$	3.26	0.1341	$0.648\ \|H\text{-}1 \rightarrow H\rangle\ 0.297\ \|H\text{-}2 \rightarrow H\rangle$
	0	4.24	0.0216	$0.502\ \|H \rightarrow L\rangle\ 0.488\ \|H \rightarrow L+1\rangle$	6.18	0.5893	$0.495\ \|H\text{-}1 \rightarrow L\rangle\ -0.490\ \|H \rightarrow L\rangle$
		4.21	0.0193	$-0.764\ \|H\text{-}1 \rightarrow L+1\rangle\ 0.284\ \|H \rightarrow L\rangle$	6.13	0.5533	$0.727\ \|H\text{-}1 \rightarrow L+1\rangle\ -0.284\ \|H \rightarrow L\rangle$
SQ	−2	2.93	0.1743	$0.874\ \|H \rightarrow L\rangle\ -0.220\ \|H\text{-}1 \rightarrow L+1\rangle$	5.13	0.3191	$-0.874\ \|H \rightarrow L\rangle\ 0.245\ \|H \rightarrow L+1\rangle$
		2.93	0.1743	$-0.562\ \|H\text{-}1 \rightarrow L\rangle\ -0.349\ \|H\text{-}1 \rightarrow H\rangle$	5.13	0.3191	$0.562\ \|H\text{-}1 \rightarrow L\rangle\ 0.349\ \|H\text{-}1 \rightarrow H\rangle$
	−1	1.51	0.0036	$-0.892\ \|H\text{-}1 \rightarrow H\rangle\ 0.132\ \|H\text{-}1 \rightarrow L\rangle$	2.83	0.1531	$-0.892\ \|H\text{-}1 \rightarrow H\rangle\ 0.132\ \|H\text{-}1 \rightarrow L\rangle$
		1.51	0.0036	$-0.740\ \|H\text{-}3 \rightarrow H\rangle\ -0.422\ \|H\text{-}1 \rightarrow L\rangle$	2.83	0.1531	$0.740\ \|H \rightarrow L+1\rangle\ 0.422\ \|H\text{-}1 \rightarrow L\rangle$
	0	2.48	0.0178	$0.960\ \|H \rightarrow L\rangle\ -0.165\ \|H\text{-}1 \rightarrow H\rangle$	4.99	0.2282	$-0.960\ \|H \rightarrow L\rangle\ -0.165\ \|H\text{-}1 \rightarrow H\rangle$
		2.48	0.0178	$-0.628\ \|H\text{-}1 \rightarrow L\rangle\ 0.484\ \|H\text{-}3 \rightarrow L\rangle$	4.99	0.2282	$-0.628\ \|H\text{-}1 \rightarrow L\rangle\ -0.484\ \|H\text{-}3 \rightarrow L\rangle$
IQ	−2	1.91	0.1679	$0.824\ \|H \rightarrow L\rangle\ -0.351\ \|H \rightarrow L\rangle$	1.91	0.1679	$0.817\ \|H \rightarrow L\rangle\ 0.354\ \|H \rightarrow L\rangle$
		2.01	0.1817	$0.824\ \|H \rightarrow L\rangle\ -0.351\ \|H \rightarrow L\rangle$	2.01	0.1817	$0.817\ \|H \rightarrow L\rangle\ 0.354\ \|H \rightarrow L\rangle$
	−1	1.73	0.0335	$-0.715\ \|H\text{-}1 \rightarrow H\rangle\ 0.387\ \|H \rightarrow L\rangle$	1.97	0.0628	$-0.827\ \|H\text{-}1 \rightarrow H\rangle\ -0.213\ \|H\text{-}1 \rightarrow L\rangle$
		1.65	0.0261	$-0.789\ \|H \rightarrow L\rangle\ -0.463\ \|H\text{-}1 \rightarrow H\rangle$	1.99	0.0757	$-0.868\ \|H \rightarrow L\rangle\ -0.236\ \|H{-}1{\rightarrow}H\rangle$
	0	3.00	0.0582	$0.855\ \|H \rightarrow L\rangle\ 0.370\ \|H\text{-}3 \rightarrow L\rangle$	5.10	0.3265	$-0.973\ \|H \rightarrow L\rangle\ 0.083\ \|H\text{-}2 \rightarrow L+1\rangle$
		2.82	0.0735	$-0.801\ \|H \rightarrow L+1\rangle\ -0.295\ \|H\text{-}2 \rightarrow L\rangle$	5.45	0.1683	$0.887\ \|H \rightarrow L+2\ \rangle\ -0.240\ \|H\text{-}2 \rightarrow L\rangle$

[a] Contributions are labeled according to the convention H = HOMO, L = LUMO, L + 1 = next in energy to LUMO and so on.

In Table 5 we show a summary of main CI contributions to the absorption threshold (first optically active electronic transition) and to the highest peak (strongest active electronic transition) from ZINDO calculations for IQ, SQ, and HQ and their negative ions. As we can see from the table, the transitions are dominated by a few configurations involving frontier orbitals, and as mentioned before, these are π-type orbitals. One interesting feature is that, as anticipated from the DM data, there are considerable changes in terms of electronic transitions considering the fully optimized and planar-constrained structures. These results suggest that we could expect significant bathochromic effects for these compounds. This aspect will be discussed in more detail when we analyze the dimeric structures.

There is strong experimental evidence from X-ray studies[21] that eumelanins present stacked planar portions similar to those observed for graphite. The presence of large planar structures contributes to π-delocalization and consequently to the decrease of the optical gap. Also, the polymerization process naturally induces a red shift of the energy gap, so we may expect overall lowering of the band-to-band transitions compared to the first absorption of a monomer. Furthermore, considering that there is a significant energetic gain under electronic capture and considering the well-known fact that there are electrons available in the biological process of eumelanin synthesis, we can expect a nonnegligible number of anions present in the samples. This implies that we may also expect the threshold of absorption to be related not to the band-to-band transitions but to transitions involving the trapped electrons or, in other words, to the absorption we show for the singly negative monomers.

The results we obtained for the monomers (neutral and ions) are thus in very good agreement with the experimental data and are fully consistent with the semiconductor models proposed for eumelanins.[23]

4. Summary and Conclusions

We have carried out ab initio, PM3, and ZINDO−CI calculations on neutral and charged 5,6-indolequinone (IQ) molecules and its reduced forms semiquinone (SQ) and hydroquinone (HQ), believed to be the main monomers of the biological pigment eumelanin.[1−3] Our results for the optical absorpion properties of these monomers are in good agreement with the data for eumelanins and so generally support this hypothesis.

Our results suggest further that these molecules are good electron acceptors. This is the first theoretical support for energetic stabilization under electronic capture based on all-electron sophisticated methods. From previous studies[17−19,24,36] only SQ was believed to be an electron acceptor. The electronic capture-and-trapping process could be the basis for an efficient protective cellular mechanism against (potentially cytotoxic) free radicals produced by metabolic dejects or ionizing radiation.

The process of polymerization and the relative energetic cost of dimerization for the many possible structural structures will be discussed in the following paper.

Acknowledgment. This work has been supported in part by the Brazilian Agencies FAPESP, FINEP, CNPq, and CAPES. We are indebted to Professor M. C. Zerner for kindly making available the ZINDO code. We thank the Laboratório de Computação Científica Avançada (LCCA-USP) for computational facilities.

References and Notes

(1) Prota, G. *Melanins and Melanogenesis*; Academic Press: New York, 1992.
(2) Swan, G. A. *Ann. N.Y. Acad. Sci*. **1963**, *100*, 1005.
(3) Swan, G. A. *Fortschr. Chem. Org. Naturst*. **1974**, *31*, 522.
(4) D'Ischia, M.; Napolitano, A.; Prota, G. *Gazz. Chim. Ital.* **1996**, *126*, 783.
(5) Nicolaus, R. A. *Melanins*; Herman: Paris, 1968.
(6) Napolitano, A.; Palumbo, A.; D'Ischia, M.; Prota, G. *J. Med. Chem*. **1996**, *39*, 5192.
(7) Jellinger, K.; Jirasek, A. *Acta Neuropathol.* **1971**, *17*, 553.
(8) Chedekel, M. R. *Photochem. Photobiol.* **1982**, *35*, 881.
(9) Giacomoni, P. U. *J. Photochem. Photobiol. B* **1996**, *29*, 87.
(10) McGinness, J. E. *Science* **1973**, *177*, 896.
(11) Proctor, P.; McGinness, J. E.; Corry, P. *Science* **1974**, *183*, 853.
(12) Strzelecka, T. *Physiol. Chem. Phys*. **1982**, *14*, 223.
(13) McGinness, J. E. *J. Theor. Biol.* **1973**, *48*, 19.
(14) Proctor, P.; McGinness, J. E.; Corry, P. *J. Theor. Biol.***1974**, *183*, 853.
(15) Blois, M. S. In *Solid State Biophysics*; Wyard, S. Y., Ed.; McGraw-Hill: New York, 1969; p 243.
(16) Galvão, D. S.; dos Santos, D. A.; Laks, B.; de Melo, C. P.; Caldas, M. J. *Phys. Rev. Lett.* **1989**, *63*, 786;
(17) Galvão, D. S.; Caldas, M. J. *J. Chem. Phys.* **1988**, *88*, 4088.
(18) Galvão, D. S.; Caldas, M. J. *J. Chem. Phys.* **1990**, *92*, 2630.

(19) Galvão, D. S.; Caldas, M. J. *J. Chem. Phys.* **1990**, *93*, 2848.
(20) Rosei, M. A.; Mosca, L.; Galluzzi, F. *Synth. Met.* **1996**, *76*, 331.
(21) Thathachari, Y. T. *Pigm. Cell* **1976**, *3*, 64.
(22) Mason, H. S. In *Advances in the Biology of Skin*; Pergamon: Oxford, 1967; Vol. 3, 293.
(23) Longuet-Higgins, H. C. *Arch. Biochem. Biophys.* **1960**, *86*, 231.
(24) Pullman, A.; Pullman, B. *Biochim. Biophys. Acta* **1961**, *54*, 384.
(25) Blois, M. S.; Zahlan, A. B.; Maling, J. E. *Biophys. J.* **1964**, *4*, 471.
(26) Frisch, M. J.; Trucks, G. W.; Schlegel, H. B.; Gill, P. M. W.; Johnson, B. G.; Robb, M. A.; Cheeseman, J. R.; Keith, T.; Petersson, G. A.; Montgomery, J. A.; Raghavachari, K.; Al-Laham, M. A.; Zakrzewski, V. G.; Ortiz, J. V.; Foresman, J. B.; Cioslowski, J.; Stefanov, B. B.; Nanayakkara, A.; Challacombe, M.; Peng, C. Y.; Ayala, P. Y.; Chen, W.; Wong, M. W.; Andres, J. L.; Replogle, E. S.; Gomperts, R.; Martin, R. L.; Fox, D. J.; Binkley, J. S.; Defrees, D. J.; Baker, J.; Stewart, J. P.; Head-Gordon, M.; Gonzalez, C.; Pople, J. A. *Gaussian 94*, revision E.2; Gaussian, Inc.: Pittsburgh, PA, 1995.
(27) Dewar, M. J. S.; Thiel, W. *J. Am. Chem. Soc.* **1977**, *99*, 4899.
(28) Dewar, M. J. S.; Zoebisch, E. G.; Healy, E. F.; Stewart, J. J. P. *J. Am. Chem. Soc.* **1985**, *107*, 4433.
(29) Stewart, J. J. P. *J. Comput. Chem.* **1989**, *10*, 209.
(30) Stewart, J. J. P. *J. Comput. Chem.* **1990**, *11*, 221.
(31) Bucci, P.; Longeri, M.; Veracini, C. A.; Lunazzi, L. *J. Am. Chem. Soc.* **1994**, *96*, 1305.
(32) Ridley, J.; Zerner, M. *Theor. Chem. Acta* **1973**, *32*, 111.
(33) Ridley, J.; Zerner, M. *Theor. Chem. Acta* **1976**, *42*, 223.
(34) Ridley, J.; Zerner, M. *Theor. Chem. Acta* **1987**, *72*, 347.
(35) Dos Santos, D. A.; Galvão, D. S.; Laks, B.; dos Santos, M. C. *Chem. Phys. Lett.* **1991**, *184*, 579 and references.
(36) Pullman, B.; Pullman, A. *Quantum Biochemistry*; John Wiley & Sons: New York, 1963.